Inversion-recovery echo-planar MR in adult brain neoplasia.

S Sheppard, P C Davis, G Kater and J E Peterson

AJNR Am J Neuroradiol 1998, 19 (2) 267-273
http://www.ajnr.org/content/19/2/267

AJNR Am J Neuroradiol 19:267–273, February 1998

Inversion-Recovery Echo-Planar MR in Adult Brain Neoplasia

Scott Sheppard, Patricia C. Davis, Gabrielle Kater, and Jack E. Peterson

PURPOSE: **A T1-weighted multishot inversion-recovery (IR) echo-planar MR imaging (EPI) sequence was developed to improve intracranial tissue differentiation; its diagnostic utility was compared with that of conventional axial T1-weighted spin-echo and axial T2-weighted turbo spin-echo sequences.**

METHODS: **Eighteen patients with known or suspected primary or metastatic brain neoplasia were imaged in a 1.5-T unit with IR-EPI sequences. Three observers measured gray/white matter contrast-to-noise ratios and subjectively compared IR-EPI sequences with T1-weighted spin-echo and T2-weighted turbo spin-echo sequences for gray/white matter discrimination, visibility of intracranial and vascular structures, overall lesion conspicuity, size of lesion(s), and presence and severity of artifacts.**

RESULTS: **Twenty-four lesions (including neoplasia, infarction, treatment-associated encephalomalacia, nonneoplastic white matter signal abnormalities, and basilar artery dolichoectasia) were detected in 12 patients. Basilar artery dolichoectasia was not included in subsequent statistical analysis. Pulsatile flow artifacts were markedly reduced on IR-EPI sequences relative to those on T1-weighted spin-echo sequences. Gray/white matter contrast was greater on IR-EPI images than on T1-weighted spin-echo images. Periaqueductal gray matter, basal ganglia, optic tracts, cranial nerve V, and claustrum were seen better or as well on IR-EPI images as compared with T1-weighted spin-echo images. IR-EPI was more sensitive to magnetic sensitivity effects, with resultant decreased visibility of cranial nerves VII and VIII and the orbital portion of the optic nerves. For noncontrast sequences, lesion conspicuity was better on IR-EPI images than on T1-weighted spin-echo images in 16 (70%) of 23 lesions and was equal on the two sequences in seven (30%) of 23 lesions. Lesion size, including surrounding edema, was greater on IR-EPI images than on T2-weighted turbo spin-echo images in two (9%) of 23 cases and equal in 21 (91%) of 23 cases. Hyperintense foci of methemoglobin were more conspicuous on T1-weighted spin-echo images.**

CONCLUSION: **Multishot IR-EPI is superior to conventional T1-weighted spin-echo imaging for parenchymal tissue contrast and lesion conspicuity, and is equal to T2-weighted turbo spin-echo imaging in sensitivity to pathologic entities.**

Traditional inversion-recovery (IR) sequences require long acquisition times (typically more than 10 minutes), which limit the applicability of this magnetic resonance (MR) technique. With the development and refinement of multishot echo-planar imaging (EPI) and fast (or turbo) spin-echo imaging sequences (1), in which several lines of k-space are acquired during each repetition time (TR), it is possible to reduce significantly the acquisition time necessary for IR sequences. For example, an IR multishot EPI sequence with five lines in k-space per TR has a scan time of 3:21 minutes. A comparable IR fast spin-echo sequence with four lines of k-space per TR has a scan time of 4:03 minutes. In contrast, the acquisition time for a conventional IR spin-echo sequence would be 16:21 minutes, assuming comparable acquisition parameters.

EPI sequences are generated by an oscillating readout gradient. While echo formation in an IR-EPI sequence is a result of a 180/90/180 radio-frequency pulse train, the actual lines in k-space for each image are sampled as a series of gradient echoes. Because of $T2^*$ decay, there is an inherent filtering of the high-frequency lines of k-space during single-shot EPI se-

Received January 3, 1997; accepted after revision August 18.

From the Department of Radiology (S.S., P.C.D., G.K., J.E.P.) and the Frederik Philips MR Research Center (S.S.), Emory University School of Medicine, Atlanta, Ga, and Philips Medical Systems, Shelton, Conn (S.S.).

Address reprint requests to Scott Sheppard, Department of Radiology, Emory University Hospital, 1364 Clifton Rd, NE, Atlanta, GA 30322.

quences. This change in signal amplitude causes significant image blurring in the phase-encoded direction during long-readout gradient periods. The trade-off for readout periods of shorter duration is reduced spatial resolution. Hence, in most single-shot EPI acquisitions, spatial resolution is limited to a maximum matrix size of 64 × 64 or 128 × 128, depending on scanner hardware performance specifications. While this resolution may be acceptable for certain functional MR applications, it is not adequate for clinical anatomic imaging (2). By using multishot imaging techniques, in which k-space is broken up into several sections and each section is scanned during subsequent TRs, improved spatial resolution can be achieved.

In this study, we optimized such a rapid, high-resolution strongly T1-weighted multishot IR-EPI sequence for brain imaging and compared it prospectively with conventional T1-weighted spin-echo and T2-weighted fast spin-echo images in a cohort of patients with known or suspected brain neoplasia.

Methods

A prospective study was completed of 18 patients, 12 with suspected brain metastases and six with known brain neoplasia. Patients' ages ranged from 21 to 77 years, with a mean age of 51 years.

All subjects underwent routine MR imaging that consisted of a sagittal scout localizer image, an axial T1-weighted (500/16/1 [TR/echo time/excitations]) spin-echo sequence (scan time, 3:53 minutes), and an axial T2-weighted (3500/120) turbo spin-echo sequence (echo train length of 12 and acquisition time of 2 minutes 6 seconds). All studies were obtained on a commercially available 1.5-T unit. After giving informed consent for contrast administration, all patients received 0.1 mM/kg of gadopentetate dimeglumine intravenously and underwent contrast-enhanced T1-weighted spin-echo imaging. Four patients had contrast-enhanced on-resonance magnetization-transfer-contrast (MTC) T1-weighted spin-echo imaging in place of conventional contrast-enhanced T1-weighted spin-echo imaging. However, we did not focus our data acquisition and study protocol to include contrast-enhanced MTC sequences formally in all patients examined for known or suspected metastatic disease.

The IR-EPI sequences were completed using scan geometry identical to that of the routine sequences. Parameters were 1500/30, an inversion time (TI) of 400, a matrix size of 256 × 204, five lines in k-space per shot, spectral fat suppression, 24 sections, each 5-mm thick with a 1-mm intersection gap, and an acquisition time of 3 minutes 21 seconds. To optimize image contrast, real rather than conventional modulus images were used with the IR-EPI sequence. All patients had noncontrast IR-EPI studies; after contrast administration, 13 patients had additional IR-EPI studies after completing either a T1-weighted spin-echo study (n = 9) or an on-resonance MTC T1-weighted spin-echo study (n = 4). Five patients refused additional MR imaging, which precluded acquisition of the postcontrast IR-EPI sequence.

Our initial efforts to optimize IR-EPI sequences included trials of IR-EPI sequences without fat suppression. These non–fat-suppressed images were severely degraded by chemical-shift artifacts. Spectral presaturation was then incorporated into the IR sequence to reduce the high-signal-intensity artifacts associated with lipid/soft tissue interfaces. The result was marked improvement in intracranial image quality at the expense of extracranial anatomic detail.

Image measurements and ratings were made using a standalone workstation; no hard copy images were used. For each identified lesion, images were compared with respect to lesion conspicuity and size only. The images of interest were displayed side by side on the workstation in a two-on-one display format with windowing and leveling parameters optimally adjusted for the unique characteristics of each image. Size discrimination was based on visual impressions.

Gray/white matter contrast comparisons were completed using noncontrast IR-EPI and T1-weighted spin-echo measurements of regions of interest localized to the head of the caudate nucleus and genu of the corpus callosum. Subjective image ratings were completed by consensus of three experienced observers using a three-point scoring system (+1 = IR-EPI diagnostically superior to compared sequence; 0 = IR-EPI equal to compared sequence; −1 = IR-EPI diagnostically inferior to compared sequence). Subjective ratings included a comparison of precontrast IR-EPI to T1-weighted spin-echo imaging with respect to gray/white matter discrimination based on conspicuity of periaqueductal gray matter and delineation of basal ganglia; visibility of small intracranial structures, such as cranial nerves II, V, VII, and VIII and claustrum; visibility of vascular structures, including basilar artery, circle of Willis, and sagittal sinus; overall lesion conspicuity; and size of lesion(s). The presence and severity of artifacts due to pulsatile flow, chemical shift, or magnetic susceptibility effects were also recorded. For each identified lesion, IR-EPI and T2-weighted turbo spin-echo images were compared with respect to lesion conspicuity and size only. Contrast-enhanced IR-EPI and T1-weighted spin-echo or MTC T1-weighted spin-echo images that showed any brain abnormalities were compared for degree of lesion enhancement, conspicuity, and size.

Results

Six of 18 patients had no brain abnormalities at MR imaging, whereas 12 patients had a total of 24 lesions. Lesions included neoplasia (n = 11; 46%), infarction (n = 6; 25%), treatment-associated encephalomalacia (n = 2; 8%), nonneoplastic white matter signal abnormalities, most likely the result of microvascular age-related changes (n = 4; 17%), and basilar artery dolichoectasia (n = 1; 4%). The basilar artery dolichoectasia lesion was not included in subsequent statistical analysis.

Region-of-interest contrast measurements between gray and white matter revealed substantially higher contrast on IR-EPI sequences (mean, 4.92 ± 1.20) than on T1-weighted spin-echo sequences (mean, 2.78 ± 0.85).

For noncontrast images, observers found that lesion conspicuity was better on IR-EPI images than on T1-weighted spin-echo images in 16 (70%) of 23 cases and equal in seven (30%) of 23 cases (Fig 1). Lesions were larger on IR-EPI studies in 13 cases (57%) and equal in 10 cases (43%), most likely related to increased conspicuity of surrounding vasogenic edema on the IR-EPI images. In comparisons of precontrast IR-EPI sequences with T2-weighted turbo spin-echo sequences, lesion conspicuity was better on the IR-EPI studies in three cases (13%), equal in 18 cases (78%), and worse in two cases (9%). Lesion size, including surrounding edema, was greater on IR-EPI studies than on T2-weighted turbo spin-echo studies in two cases (9%) and equal in 21 cases (91%) (Fig 2).

FIG 1. An unenhancing recurrent tumor nodule within the medial left temporal lobe is seen better on noncontrast IR-EPI image (*arrow, A*) than on noncontrast T1-weighted spin-echo image (*B*). For comparison, the postcontrast IR-EPI image (*C*) shows no lesion contrast enhancement. Postoperative encephalomalacia of the anterior left temporal lobe is seen equally well on IR-EPI and T1-weighted spin-echo images.

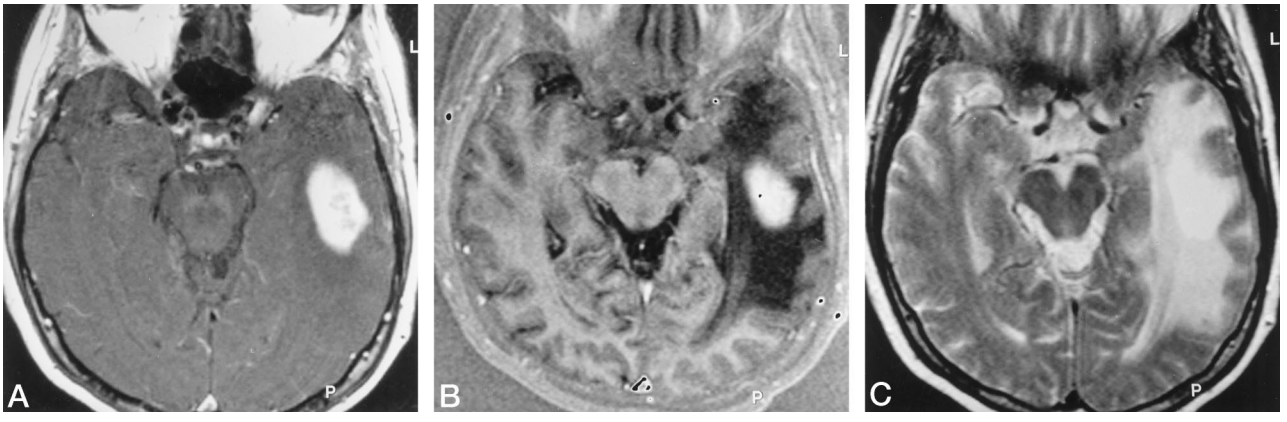

FIG 2. Although an area of solid tumor enhancement in the left temporal lobe is similarly apparent on the T1-weighted spin-echo image with on-resonance MTC (*A*) and the IR-EPI image (*B*), the surrounding vasogenic edema is much more apparent on the IR-EPI image. Depiction of vasogenic edema with the IR-EPI sequence approaches that of the T2-weighted turbo spin-echo image (*C*).

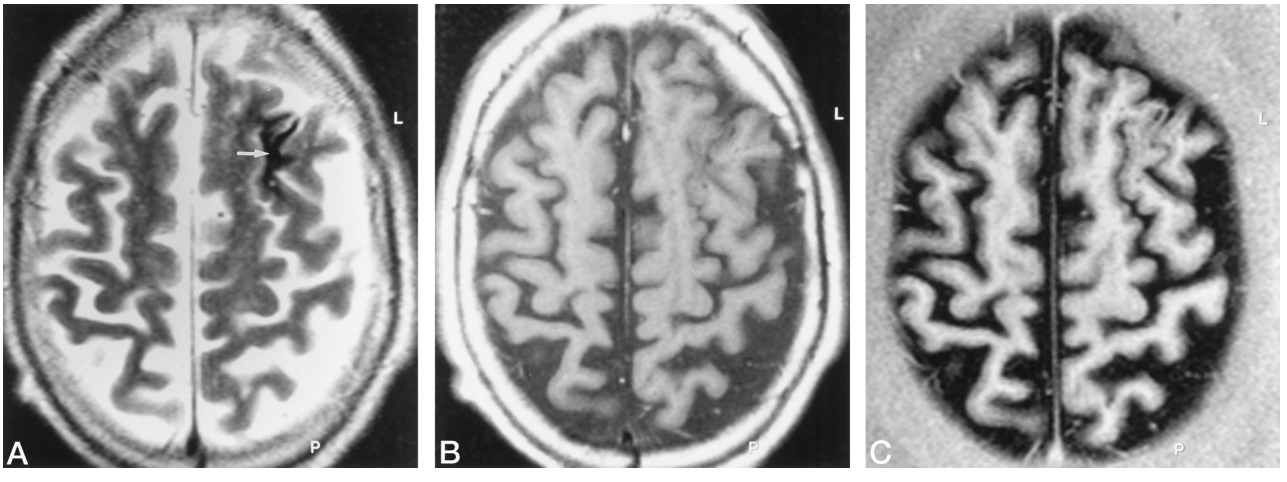

FIG 3. A hypointense gyriform lesion was thought to contain hemosiderin or other cations because of its appearance on the T2-weighted turbo spin-echo study (*arrow, A*). As expected, this finding was not seen on either the noncontrast T1-weighted spin-echo image (*B*) or the IR-EPI image (*C*).

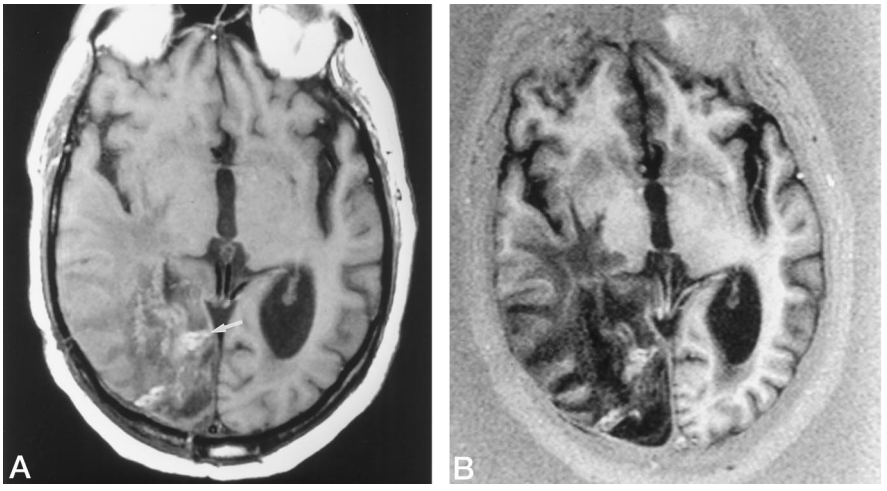

FIG 4. A focal area of hyperintense signal within an area of tumor was suggestive of methemoglobin on noncontrast T1-weighted spin-echo image (*arrow, A*). On the noncontrast IR-EPI image (*B*), this area has a signal intensity similar to that of white matter, thus representing a potential pitfall of IR-EPI.

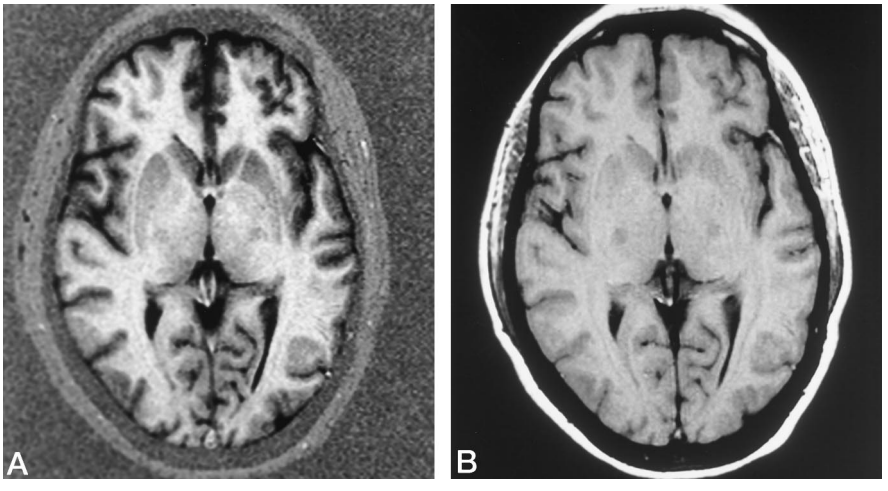

FIG 5. The contrast between gray matter and white matter as evidenced by the margins of the claustrum, internal capsule, and basal ganglia is significantly improved on the IR-EPI sequence (*A*) as compared with the conventional T1-weighted spin-echo image (*B*).

Among the 13 subjects who had postcontrast IR-EPI studies, 19 lesions were noted, of which seven enhanced. Conspicuity and size were greater on the postcontrast IR-EPI studies than on the postcontrast T1-weighted spin-echo or MTC T1-weighted spin-echo studies in 13 (68%) of the 19 lesions and similar in six (32%). For the seven enhancing lesions, six (86%) showed similar enhancement on IR-EPI and T1-weighted spin-echo or MTC T1-weighted spin-echo studies (Fig 2), while one lesion was less intense on IR-EPI sequences than on T1-weighted spin-echo sequences.

Six lesions contained foci that had signal intensities suggestive of intralesional blood products (methemoglobin, hemosiderin, or other blood/proteinaceous complexes). Since no patient in this study had a history of melanoma, it is unlikely that the foci were due to the presence of melanin. Four lesions were hypointense on T2-weighted turbo spin-echo images and contained no hyperintense regions on T1-weighted spin-echo or IR-EPI studies (Fig 3). Two lesions had hyperintense foci characteristic of methemoglobin on T1-weighted spin-echo images; one of these was isointense with normal white matter on IR-EPI studies and hence inconspicuous (Fig 4).

In all cases the periaqueductal gray matter and basal ganglia were delineated better on IR-EPI than on T1-weighted spin-echo images (Fig 5). Likewise, in 14 (73%) of 19 cases, the claustrum was seen better with IR-EPI than with T1-weighted spin-echo imaging. The cisternal portions of the cranial nerves were generally depicted better on T1-weighted spin-echo images than on IR-EPI studies (cranial nerves VII and VIII, 16/19, 84%; cranial nerve V, 9/19, 47%). Although in all cases the optic tracts were seen as well or better on IR-EPI sequences relative to T1-weighted spin-echo sequences, the intraorbital optic nerves were poorly seen on IR-EPI studies.

For vascular structures, the basilar artery, circle of Willis, and major venous sinuses were well demonstrated on IR-EPI in the majority of cases. Flow-associated image artifacts were markedly reduced on IR-EPI, particularly in the posterior fossa (Fig 6). While the multishot IR-EPI sequence resulted in a marked improvement in brain imaging, particularly near the skull base, magnetic susceptibility artifacts essentially obscured anatomic detail of most extracranial structures (orbit, paranasal sinus, temporal bone, Fig 7).

FIG 6. Multiple small cerebellar infarctions are obscured by pulsation artifact on the postcontrast T1-weighted spin-echo image (*A*). A reduction in flow-related artifacts with IR-EPI renders these foci visible (*arrows, B*). Note also that the normal medulla is distorted by flow artifacts on *A* as compared with *B*. Encephalomalacia on the parasagittal T1-weighted spin-echo image (*arrow, C*) confirms a left-sided cerebellar infarction.

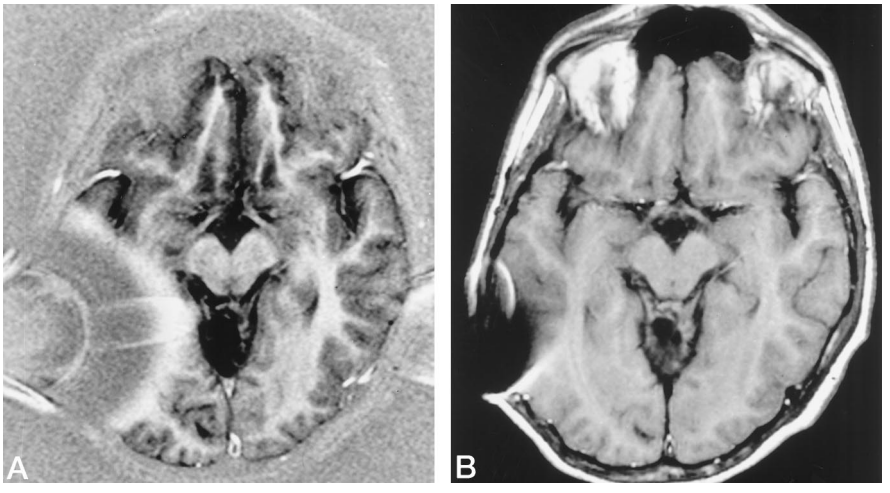

FIG 7. Magnetic susceptibility artifact corresponding to a shunt catheter in the right temporal region severely impedes visibility of the adjacent brain on the IR-EPI sequence (*A*). The artifact is present but less troublesome on the T1-weighted spin-echo image (*B*).

Discussion

Conventional spin-echo and gradient-echo images generate only positive longitudinal magnetization, and as such are displayed as modulus images that do not discriminate the sign of longitudinal magnetization. A modulus image is produced from the square root of the sum of the squares of the real and imaginary images. Thus, if there were any negative longitudinal magnetization present in the real or imaginary image, this magnetization would not be apparent in the modulus image. As a result, the attendant contrast generated in a modulus image can only range from 0 to +1.

On the other hand, IR sequences rotate the longitudinal magnetization into the negative magnetization axis. As such, with proper choice of TR (infinite, as in single-shot EPI, or if TR much is greater than TI), echo time, and TI, it is possible to generate contrast with a range of $-(1-e^{-TR/T1})$ to $+(1-e^{-TR/T1})$ (3), thereby yielding superior T1 contrast relative to a short-TR/short-echo-time spin-echo sequence. To display this improved contrast, a real image must be substituted for the modulus image. With the use of real images, a tissue that has no longitudinal magnetization (ie, air, bone, or suppressed fat) will have medium-gray signal intensity. Tissue with a positive magnetization, such as white matter, will be light gray in intensity, and negative magnetization tissues, such as gray matter, will be dark gray. Water or cerebrospinal fluid will appear as very low intensity, or black. To depict the full range of image contrast offered by the IR-EPI sequences, we considered only IR real images in this study.

IR sequences using conventional MR technology have proved useful for optimization of contrast of gray/white matter in the brain (4), for fat-suppressed imaging (known as short-tau IR or STIR) (5), and, more recently, for fluid-suppressed imaging (known as fluid-attenuated inversion recovery, or FLAIR) (6). Our initial experience with IR sequences with echo-planar technology was disappointing, however, primarily because of marked image degradation from chemical-shift artifacts. In a classic spin-echo or gradient-echo sequence, in which only one phase-encode gradient is applied per TR, these errors are irrelevant. Because EPI sequences use a blipped phase-encoding gradient scheme, the resulting images are more sensitive to significant chemical-shift artifacts (7). Owing to the difference in resonance frequency between water and fat (about 220 Hz at 1.5 T), small phase

errors can be created. With the blipped phase-encode gradient used in our EPI sequence, these phase errors propagate additively as a function of the number of lines of k-space acquired during a given TR. As a result, significant chemical-shift errors exceeding five pixels can be produced with EPI. In this study, the inversion delay was optimized for gray/white matter contrast rather than for fat suppression, as in a short-tau IR sequence. Therefore, a spectral fat-suppression pulse was used in order to reduce the chemical-shift artifacts created on EPI brain images by skull base and facial fat.

With single-shot EPI, magnetic susceptibility artifacts can be a major cause of reduced image quality and overt signal loss. For this reason, single-shot EPI has not been very successful when imaging the skull base (8). With multishot EPI, the echo train length is much shorter than for a single-shot acquisition, which, in the present case, was five. Consequently, the magnitude of magnetic susceptibility artifacts in this study was much less than that obtained with single-shot EPI.

The choice of TI has a dramatic effect on image contrast. Longitudinal relaxation times or T1 relaxation values change depending on magnetic field strength. In this study, the TI was optimized for 1.5-T imaging such that gray matter was hypointense relative to background (air) and white matter was hyperintense relative to background. If instead we had chosen to use a substantially shorter TI, such that the longitudinal magnetization of white matter was reduced, the expected result is that some contrast between white matter and gray matter would remain but the degree of contrast would decrease. Therefore, a comparison of our results with IR protocols with significantly different TI values and different field strengths without adjusting the TI for the field strength could be misleading. Likewise, different tissues and attendant abnormalities also have different T1 relaxation times. In this study, the choice of TI was governed by a desire to maximize gray/white matter contrast. It is conceivable that different values of TI/TR and echo time would improve tumor/tissue contrast.

The primary clinical advantages demonstrated in this study of IR-EPI are its rapid acquisition time compared with conventional and fast IR sequences, which are based on conventional MR technology; reduction of pulsatile flow artifacts, especially in the posterior fossa; and improved T1 image contrast. This study confirmed that with IR-EPI we can reduce acquisition times by 80% and 21% as compared with IR spin-echo or IR fast spin-echo sequences, respectively. It is possible that IR fast spin-echo protocols can be created with scan times equal to those reported for this multishot IR-EPI study. However, as improved gradient technology becomes available, it is probable that shorter scan times for IR-EPI can be achieved by acquiring more lines of k-space per TR (ie, k-space trajectories or shots) as well.

Our preliminary findings suggest that one practical potential role for IR-EPI is in achieving improved contrast resolution for lesions in proximity to major vascular structures, especially those located in the posterior fossa. With IR-EPI, flow-associated artifacts were greatly reduced or inapparent on both noncontrast and contrast-enhanced sequences. Although further investigation of this phenomenon is warranted, this finding may stem from the very short time between each readout gradient lobe associated with the oscillating readout gradient used in EPI. This could have allowed less time for flow-related phase errors to accumulate with a secondary reduction in the severity of flow-related image artifacts. At present, successful reduction of flow artifacts with conventional MR technology has been problematic, especially after paramagnetic contrast administration. Although the addition of flow-compensation gradient pulses is effective in reducing flow-related artifacts for T2-weighted sequences, the lengthened echo time required to apply flow-compensation gradients lessens depiction of T1-shortening associated with contrast enhancement.

We found that IR-EPI offers superior contrast discrimination for anatomic detail and for lesion characterization as compared with T1-weighted spin-echo imaging. A somewhat surprising finding was the successful comparisons of IR-EPI with T2-weighted turbo spin-echo imaging for lesion size and conspicuity, indicating a greater sensitivity of IR-EPI to tissue abnormalities than has traditionally been achieved with T1-weighted sequences. Because most pathologic lesions and associated vasogenic edema have a higher water content than normal brain tissue, it is not entirely unexpected that the large negative magnetization induced by the IR-EPI sequence would appear as an area of low signal intensity (ie, black) on IR-EPI images. The greater dynamic range of IR-EPI in combination with a higher water content accounts for the improved visibility of hypointense vasogenic edema on IR-EPI.

The major drawback of IR-EPI was a marked reduction in anatomic detail of the skull base, orbit, and adjacent extracranial tissues. Since muscle has a relatively long T1 relative to that of fat and white matter, the choice of a TI of 400 will significantly reduce its signal intensity and hence reduce visibility. Likewise, to avoid chemical-shift artifacts, spectral fat suppression was used. This further serves to reduce the visibility of all fat-containing extraaxial structures. Further, magnetic susceptibility artifacts, while not a major problem on our sequences, serve to reduce definition at air/bone and bone/soft tissue interfaces. Overall, this combination of factors (choice of TI, fat suppression, and magnetic susceptibility) leads to generally poor imaging of extraaxial structures. For this reason, this IR-EPI sequence should be used only for improved imaging of brain parenchymal detail. Conventional sequences should still be used for imaging of cisternal, calvarial, and extracranial tissues and diseases.

Another potential limitation of multishot IR-EPI is reduced contrast between high signal intensity of normal white matter and other entities that have a short

T1 relaxation time, such as enhancing or methemoglobin-containing lesions. This limitation is not unique, however, to IR-EPI sequences. Similar difficulties have been reported with other sequences that increase gray/white matter contrast and white matter signal intensity, such as gradient-echo T1-weighted volumetric acquisitions (10).

Blood vessels such as the middle cerebral artery do not always appear as flow voids; they often appear slightly hyperintense relative to background. Consequently, IR-EPI is not a reliable method to assess vascular stasis or thrombus.

Conclusion

This study of patients with known or suspected brain neoplasms established that a clinically feasible IR-EPI protocol is superior to conventional T1-weighted spin-echo sequences for demonstrating brain parenchymal tissue contrast and lesion conspicuity. IR-EPI paralleled T2-weighted turbo spin-echo imaging in sensitivity to disease and provided improved definition of the cerebellum owing to a reduction of flow artifacts. Disadvantages of IR-EPI include loss of extracranial tissue detail and the need for careful choice of window and level when filming. IR-EPI is particularly helpful in the detection of cerebellar lesions, and may have application in the study of migrational abnormalities, infarcts, and certain neoplasms, for which conventional two- and three-dimensional acquisition times are prohibitive. Since the information content is similar to T2-weighted images for intraaxial anatomy in adult patients with intraaxial neoplasms, multishot IR-EPI could serve as a replacement for T1- and T2-weighted acquisitions in situations in which scan time is at an absolute premium.

Acknowledgment

We gratefully acknowledge the assistance of Carol Ann Padgett for manuscript editing and final preparation.

References

1. Hennig J, Naverth A, Friedburg H. **RARE imaging is a fast imaging method for clinical MR.** *Magn Reson Med* 1986;3:823–833
2. Ogawa S, Tank DW, Menon R, et al. **Brain magnetic resonance imaging with contrast dependent on blood oxygenation.** *Proc Natl Acad Sci U S A* 1990;87:9868–9872
3. Hendrick RE, Raff U. **Image contrast and noise.** In: Stark DD, Bradley WG, eds. *Magnetic Resonance Imaging.* 2nd ed. St Louis, Mo: Mosby-Year Book; 1992;1:109–144
4. Johnson MA, Pennock JM, Bydder GM, et al. **Clinical NMR imaging of the brain in children: normal and neurologic disease.** *AJNR Am J Neuroradiol* 1983;141:1005–1018
5. Bydder GM, Young IR. **MR imaging: clinical use of the inversion recovery sequence.** *J Comput Assist Tomogr* 1985;4:659–675
6. DeCoene B, Hajnal JV, Gatehouse P, et al. **MR of the brain using fluid-attenuated inversion-recovery (FLAIR) pulse sequences.** *AJNR Am J Neuroadiol* 1992;13:1555–1564
7. Ordidge RJ, Coxon R, Howseman A, et al. **Snapshot head imaging at 0.5T, using the echo planar technique.** *Magn Reson Med* 1988;8:110–115
8. Siewert B, Patel MR, Mueller MF, et al. **Brain lesions in patients with multiple sclerosis: detection with echo-planar imaging.** *Radiology* 1995;196:765–771
9. Simonson TM, Magnotta VA, Ehrhardt JC, et al. **Echo-planar FLAIR imaging in evaluation of intracranial lesions.** *Radiographics* 1996;16:575–584
10. Brant-Zawadzki M, Gillan GG, Nitz WR. **MP RAGE: a three-dimensional, T1-weighted, gradient-echo sequence: initial experience in the brain.** *Radiology* 1992;182:769–775